

Time-Varying Synergies in Velocity Profiles of Finger Joints of the Hand during Reach and Grasp

Ramana Vinjamuri, Zhi-Hong Mao, Robert Scwabassi, and Mingui Sun

Abstract— This paper presents time-varying synergies that were observed during reach and grasp experiments in angular velocity profiles of metacarpophalangeal (MCP) and proximal interphalangeal (PIP) joints of five fingers of the hand. Five right handed subjects were asked to reach and grasp 28 different objects and during this experiment joint angles were measured by a data glove. Our results showed that the angular velocity profiles for a period of 0.86 seconds of ten joints (two per finger) were accurately reproduced by using only 3 synergies in 28 different tasks. Interestingly, there were correlations between the object size and velocity profiles which lead to unique distinctions in the combinations of these synergies in achieving the natural movements.

I. INTRODUCTION

THE concept of synergies has received increasing attention in motor control as it presents the two most interesting problems of coordination and dimensionality reduction by central nervous system. The study of synergies has high significance in many fields, including human computer interface and robotics. For example, in telesurgery, robotic hands are utilized to perform surgical manipulations by a surgeon at a remote site. An efficient data representation by synergies provide improved control by reducing the delay and jitter during data transmission over the network.

The term of synergy, originally coined by Bernstein [1], has been defined differently in different contexts. In the current paper, synergies in velocity profiles are defined based on the numerical interpretation by d’Avella et al. [2, 3]. Specifically, the angular velocity profile of each joint is represented as a combination of different time-varying velocity components which we define as synergies. In the literature of hand movement studies, few reports have addressed the concept of time-varying kinematic synergies observed in joint movements (e.g. [4, 5]). Postural synergies have been widely proposed where a small number of dominant postures or eigen postures can represent a large set

of postures recorded either at discrete times of a task or during different tasks [6, 7, 8]. The former case is similar to a time-varying synergy but the latter deals with static postures. Yet another concept of synergies was proposed by Todorov and Ghahramani [9] where they described using postural synergies that synergistic control may not mean dimensionality reduction or simplification, but might imply task optimization. What synergies imply, still remains debatable. In the current paper we still stress on dimensionality reduction and moving a step forward we present “time-varying” kinematic synergies in the angular velocity profiles.

As reported in literature [5], we also observed single peak velocity profiles and increased velocities at proximal joints for larger apertures. During reach and grasp, opening was observed to be faster and closing slower. More physiological implications are discussed later in section IV.

II. METHODS

A. Time-varying synergies

We model each angular velocity profile $\mathbf{v}(t)$ (consisting of rows which correspond to the angular velocity profiles of joints) as a linear combination of N movement patterns represented by $\mathbf{w}_i(t - t_{si})$, $i = 1, \dots, N$. These movement patterns are called synergies, which vary with time, with shift denoted by $t - t_{si}$ and objects denoted by subscript s . For instance, $\mathbf{w}_i(\tau)$ is a column vector that denotes the angular velocities of 10 joints at time τ for i^{th} synergy. Each angular velocity profile obtained while grasping an object is called an episode. Thus the angular velocity profile of an episode s is given by

$$\mathbf{v}_s(t) = \sum_{i=1}^N c_{si} \mathbf{w}_i(t - t_{si}) \quad (1)$$

where N refers to the number of synergies. In the above equation, c_{si} and t_{si} refer to the coefficient and time shift, respectively. They are unique for one particular synergy and one particular episode. This is illustrated in Fig. 1 where three synergies with different coefficients and shifts combine to reproduce velocities at 3 joints.

B. Materials

The experimental setup consists of CyberGlove[®] equipped with 22 sensors which can measure angles at all the finger joints including distal, proximal and metacarpal joints. For the purpose of this experiment only ten of the sensors which correspond to metacarpal (flexion/extension) and proximal

Manuscript received March 18, 2007. This work was supported by University of Pittsburgh Central Research Development Fund.

Ramana Vinjamuri is graduate research assistant working towards PhD in Department of Electrical and Computer Engineering at University of Pittsburgh.

Zhi-Hong Mao, PhD is Assistant Professor in Department of Electrical and Computer Engineering, University of Pittsburgh

Robert Scwabassi, MD, PhD is Professor of Neurological Surgery, Neuroscience, Psychiatry and Electrical, Mechanical and Biomedical Engineering, University of Pittsburgh.

Mingui Sun, PhD is Associate Professor of Neurological Surgery in the Department of Neurological Surgery and Electrical and Bio Engineering, University of Pittsburgh (mrsun@neuronet.pitt.edu).

joints of five fingers are used because distal interphalangeal joints did not move significantly. Twenty eight objects (wooden and plastic) of different shapes (spheres, circular discs, rectangles, pentagons, nuts and bolts) and different dimensions (1.5 cm–11.8 cm) were selected based on two strategies. One was gradually increasing sizes of similar shaped objects and the other was different shapes to isolate proximal and metacarpal joints. Some similar sized/shaped objects were intentionally used to observe trends in reach and grasp movements.

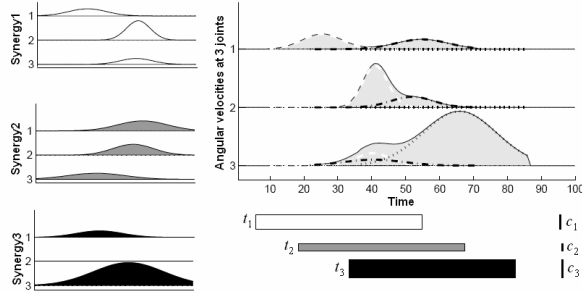


Fig. 1. An example of construction of joint velocity patterns at 3 joints by linear combination of three synergies (left) with different coefficients and shifts. The horizontal bars and vertical bars represent, respectively, the effective shifts of the synergies and the amplitude of the coefficient values. Figure adapted from [2].

C. Experiments

A typical experiment consists of reaching and grasping 28 objects. Each task has 10 trials where subjects repeated the reach and grasp for the same object 10 times. After a short recess of about 2-3 minutes, the next task was started. The start and stop times of each task were signaled by computer-generated beeps. In each task, the subject was in a seated position, resting his/her hand at corner of a table and then, upon hearing the beep, reached and grasped the object placed approximately 40 cm away on the edge of the table. Each task lasted for 2.3 seconds.

D. Analysis

After obtaining the joint angles at various times from the experiment, angular velocities were calculated. Ten trials were collected for each task. These angular velocities were filtered from noise. Since the 10 trials did not start exactly at the same time, one profile was fixed and a best match for this profile was calculated by shifting horizontally the remaining profiles, and finally they were averaged to obtain one angular velocity profile for one object. One such angular velocity profile will have ten rows corresponding to the 10 considered joints of five fingers. This process was repeated for all objects and all subjects. At the end, the obtained angular velocity profile was truncated to 0.86 s (from a total of 2.3 s) as remaining time had no useful information because velocities settled to zero by that time.

Next, the angular velocity profiles were used as inputs to a gradient descent algorithm, which is discussed in detail later in this section. We utilized a similar algorithm to that reported by d'Avella et al. [2, 3] except that we allowed

negative values in angular velocity calculation. For each subject, the collected profiles were optimized in eight cases in which different numbers of synergies from 1 to 8 were considered.

Following is the method of iterative minimization of reconstructive error. The error is given by

$$E^2 = \sum_s E_s^2 \quad (2)$$

with

$$E_s^2 = \sum_{t=1}^{T_s} \left\| \mathbf{v}_s(t) - \sum_{i=1}^N c_{si} \mathbf{w}_i(t - t_{si}) \right\|^2$$

where E is the total error, E_s refers to the error per episode, and T_s refers to the duration of an episode.

The optimization algorithm used to minimize the error is the steepest descent method with constant step size. For each subject and for each N (number of synergies), the algorithm was run five times, starting from different initial values of the synergies. Then the results (synergies) from the trial with the minimal error were used for further analysis. The strategies of choosing the initial values of synergies included: (1) random values, (2) the first or last N episodes of the angular velocity profiles, (3) average of all episodes, and (4) optimal synergies from the results obtained for $N - 1$ synergies. The amplitude coefficients started from random values between 0 and 1. The stopping criterion of the algorithm was based on the number of iterations. It was found that after 2000 iterations there was not appreciable decrease in the error in all the above cases.

For better understanding, the algorithm can be broken down to three major steps:

1) *Find optimal synergy shifts*: Compute the sum of scalar products of s^{th} episode and i^{th} synergy shifted by time t or scalar product of cross-correlation at delay t , for all possible delays. Select the synergy and delay (t_{si}) with highest cross correlation. Subtract from the data the selected synergy (after scaling and time shifting). Repeat this for remaining synergies. This completes one object/episode. Repeat the same for all remaining episodes.

2) *Update scaling coefficients*: For each episode given the synergies and delays t_{si} , update the scaling coefficients c_{si} by gradient descent.

$$\Delta c_s = -\mu_c \nabla_{c_s} E_s^2 \quad (3)$$

3) *Update synergy elements*: Given optimal shifts and updated scaling coefficients, update the synergy elements $\mathbf{w}_{i\tau} = \mathbf{w}_i(\tau)$ by gradient descent.

$$\Delta \mathbf{w}_{i\tau} = -\mu_w \nabla_{\mathbf{w}_{i\tau}} E_s^2 \quad (4)$$

After these three steps, error is calculated and iterated again until the error is reduced to a satisfactory value. For further details please refer to [2].

III. RESULTS

Using the above optimization method, encouraging results were obtained which not only lead directly to data reduction and simplification but also gave implications to physiological aspects. Fig. 2 shows three synergies which

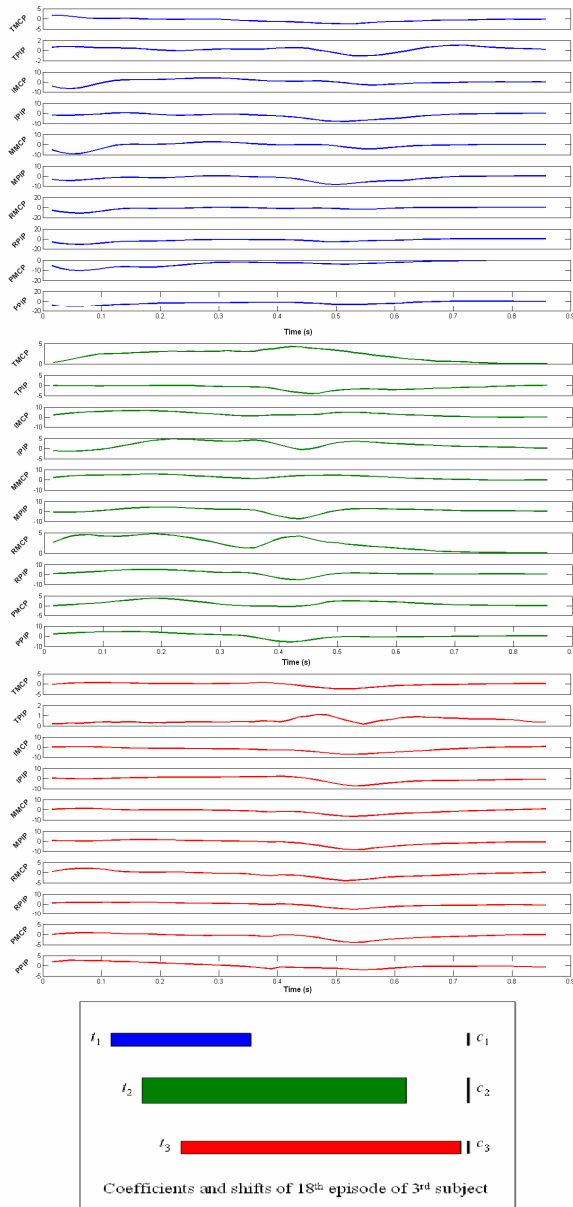


Fig. 2. Three synergies (blue, green, red) linearly combine with different time shifts and coefficients (in that order) to reproduce angular velocity patterns at ten joints. Angular velocities (rad/s) at MCP and PIP joints are shown for all five fingers from thumb (T) to pinky (P).

linearly combine with different coefficients and shifts to produce a set of ten velocity patterns of ten joints (dashed line) in a single task of reach and grasp as shown in Fig. 3. Also shown in the figure are the original patterns obtained experimentally in solid lines. The above three synergies were task-independent synergies used for 28 different tasks of object reach and grasps. Here positive and negative velocities refer to the movements in the opposite directions. Along the columns are MCP—metacarpophalangeal, PIP—

proximal interphalangeal joints of the five fingers, thumb (T), index (I), middle (M), ring (R), and pinky (P).

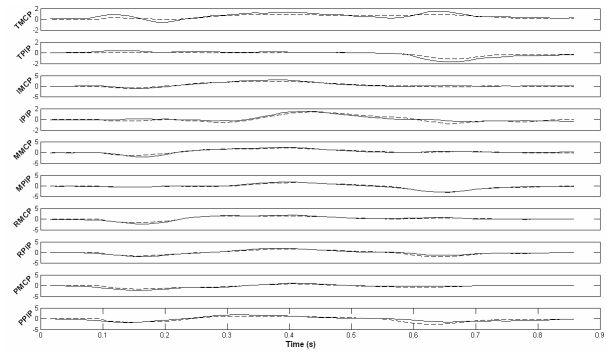


Fig. 3. Experimental angular velocity profile (—) is reproduced (---) by using the above synergies. Angular velocities (rad/s) at MCP and PIP joints are shown for all five fingers from thumb (T) to pinky (P).

As mentioned earlier eight cases differing in number of synergies (1–8) were dealt for five subjects. A mean error plot with standard deviation was obtained for all the five subjects as shown in Fig. 4 which implied that using more than three synergies did not add much significant improvement to the reproduction of the original data. Also, there was a noticeable decrease in mean error difference from 1 synergy to 2 synergies (0.7322) to that from 3 synergies to 4 synergies (0.1926).

Within a subject, in different cases with different number of synergies, correlations between synergies were measured which led us to the correlation pyramid as shown in Fig. 5. Nodes in the figure indicate synergies in different cases (e.g. 32—the second synergy in the case of three synergies). Correlations are indicated by thickness of connecting bars

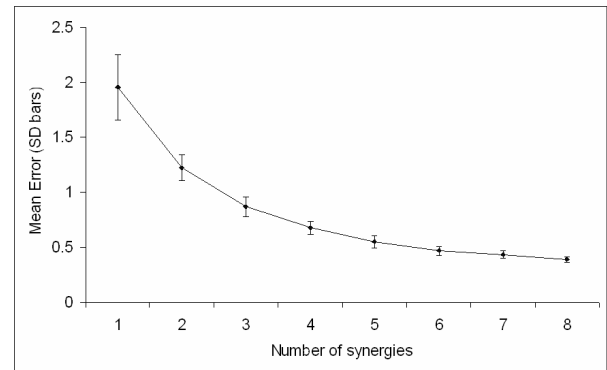


Fig. 4. Error plot illustrating sharp decrease in the error difference before 3 synergies.

between the nodes following the legend (top right). Pyramid was achieved by fixing one synergy and time-shifting the other until the best correlation was obtained (similar to *Find optimal synergy shifts* in Section II). Correlations above 0.5 only were reported in the figure and others were discarded. The correlation pyramid shown here was for one subject but similar trend was seen in all the subjects. It is clearly evident from the figure that there was high correlation between synergies in almost all the cases, except for the later ones (22, 33, 44, 55 and 66). This means as the number of synergies considered increased gradually there was a high

correlation between synergies in adjacent cases. In other words synergies in the lower cases were preserved. This ensures (with help of Fig. 4) that considering more than 3 synergies would still be consistent with 3 synergies.

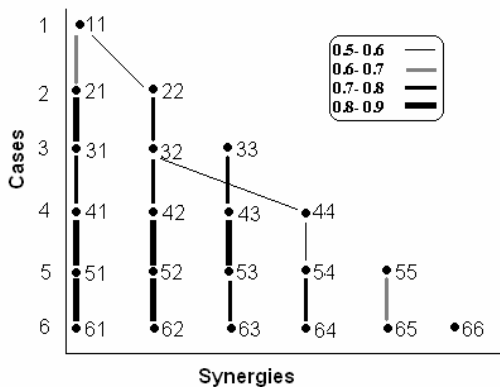


Fig. 5. Correlations of synergies depicting synergies are preserved.

IV. DISCUSSION

In quantitative analyses like principal component analysis, there exists no correlation between the components as they are orthogonal to each other. But in this approach, much similar to radial basis functions there can be similarities between the components. Though we have observed correlations between the synergies utilized in the cases where different numbers of synergies were used, the correlations were not in order. For instance, for one of the subjects, the first synergy in the case of 2 synergies was similar to second synergy in the case of 3 synergies.

From the synergies obtained, in all most all cases the outer joint of thumb was moved only at the end of the task, which indicates that thumb was used as reference throughout the task and moved in finer movements for completion of the grasp. This was verified by experimental angular velocities. During all tasks, opening was observed to be faster and closing slower which was indicated by steep rise in angular velocities during opening.

V. CONCLUSION

The successful representation of the original angular velocity profiles using synergies not only is physiological importance but also leads to a compact set of data facilitating data-traffic intensive applications. Videos of these time-varying synergies can visually explain reach and grasps. The current paper is limited only to kinematic features during a small number of reach and grasps tasks; exploring dynamic features in the more general case will make this approach more attractive because of its unique ability in data representation. Also, investigating the concept of synergies in muscle activity of the major muscles during similar experiments using surface electromyography may reveal more details about how central nervous system tackles the high degree of freedom of the hand and lead to efficient control of future electromyographic hands. We

view these as a future scope of this project.

REFERENCES

- [1] N. Bernstein, *The Co-ordination and Regulation of Movement*. Pergamon, Oxford, 1967.
- [2] A. d'Avella and M. C. Tresch, "Modularity in the motor systems: decomposition of muscle patterns as combinations of time-varying synergies," in *Advances in Neural Information Processing Systems*, vol. 14, pp. 141–148, T. G. Dietterich, S. Becker, and I. Z. Ghahraman, Eds. Cambridge, MA: MIT Press, 2002.
- [3] A. d'Avella, P. Saltiel and E. Bizzi, "Combination of muscle synergies in the construction of motor behavior," *Nature Neuroscience*, vol. 6, no. 3, pp. 300–308, 2003.
- [4] I. V. Grinyagin, E. V. Biryukova, and M. A. Maier, "Kinematic and dynamic synergies of human precision-grip movements," *J. Neurosci.*, vol. 94, pp. 2284–2294, 2005.
- [5] K. J. Cole and J. H. Abbs, "Coordination of three-joint digit movements for rapid finger-thumb grasp," *J. Neurophysiol.*, vol. 55, pp. 1407–1423, 1986.
- [6] C. R. Mason, J. E. Gomez, and T. J. Ebner, "Hand synergies during reach-to-grasp," *J. Neurophysiol.*, vol. 86, pp. 2896–2910, 2001.
- [7] M. Santello, M. Flanders, and J. F. Soechting, "Postural hand synergies for tool use," *J. Neurosci.*, vol. 18, pp. 10105–10115, 1998.
- [8] M. Santello, M. Flanders, and J. F. Soechting, "Patterns of hand motion during grasping and the influence of sensory guidance," *J. Neurosci.*, vol. 22, pp. 1426–1435, 2002.
- [9] E. Todorov and Z. Ghahramani, "Analysis of the synergies underlying complex hand manipulation," *Proc. Annu. Conf. IEEE Engineering in Medicine and Biology Society*, vol. 4, 2004.